Letter

Berezinskii-Kosterlitz-Thouless transitions in an easy-plane ferromagnetic superfluid

Andrew P. C. Underwood [1] Andrew J. Groszek [2,3] Xiaoquan Yu [4,1] P. B. Blakie [1] and L. A. Williamson [2]

[1]*Department of Physics, Centre for Quantum Science, and Dodd-Walls Centre for Photonic and Quantum Technologies, University of Otago, Dunedin, New Zealand*

[2]*ARC Centre of Excellence for Engineered Quantum Systems, School of Mathematics and Physics, University of Queensland, Saint Lucia, Queensland 4072, Australia*

[3]*ARC Centre of Excellence in Future Low-Energy Electronics Technologies, School of Mathematics and Physics, University of Queensland, Saint Lucia, Queensland 4072, Australia*

[4]*Graduate School of China Academy of Engineering Physics, Beijing 100193, China*

(Received 29 July 2022; accepted 1 March 2023; published 23 March 2023)

A two-dimensional spin-1 Bose gas exhibits two Berezinskii-Kosterlitz-Thouless (BKT) transitions in the easy-plane ferromagnetic phase. The higher-temperature transition is associated with superfluidity of the mass current determined predominantly by a single spin component. The lower-temperature transition is associated with superfluidity of the axial spin current, quasi-long-range order of the transverse spin density, and binding of polar-core spin vortices (PCVs). Above the spin BKT temperature, the component circulations that make up each PCV spatially separate, suggesting possible deconfinement analogous to quark deconfinement in high-energy physics. Intercomponent interactions give rise to superfluid drag between the spin components, which we calculate analytically at zero temperature. We present the mass and spin superfluid phase diagram as a function of quadratic Zeeman energy q. At $q = 0$ the system is in an isotropic spin phase with SO(3) symmetry. Here the fluid response exhibits a system size dependence, suggesting the absence of a BKT transition. Despite this, for finite systems the decay of spin correlations changes from exponential to algebraic as the temperature is decreased.

DOI: 10.1103/PhysRevResearch.5.L012045

Spinor Bose gases boast a plethora of spin phases, providing an ideal system for studying equilibrium and nonequilibrium properties of phase transitions [1,2]. At zero temperature a ferromagnetic spin-1 condensate with quadratic Zeeman energy $0 < q < q_0$ is in the easy-plane phase, with q_0 being a quantum critical point [3,4]. This phase exhibits two broken continuous symmetries: a U(1) symmetry associated with global phase coherence and an SO(2) symmetry associated with transverse spin coherence [5]. Quenching the system from the polar ($q > q_0$) to the easy-plane phase has revealed rich nonequilibrium dynamics as the system orders to the new ground state [6–17].

An even richer phase structure is possible at finite temperature due to the multitude of possible defects and superfluid currents [18–26]. In two dimensions (2D), it is well known that true long-range order is prohibited [27,28] and that the onset of superfluidity is instead associated with a Berezinskii-Kosterlitz-Thouless (BKT) transition [29–31]. In an easy-plane ferromagnetic spin-1 Bose gas, the two continuous symmetries give rise to two distinct BKT temperatures [25]. Beyond the existence of these transitions, however, little is known about the finite-temperature phases of this system. At $q = 0$, the order parameter manifold changes from $U(1) \times SO(2)$ to SO(3) [32]. In general, the nature of superfluidity in SO(3) systems is not well understood [25,33–37].

In this Research Letter we explore the finite-temperature behavior of a 2D spin-1 ferromagnetic Bose gas in the easy-plane phase. Results are obtained via sampling of the dynamical evolution of the system (cf. Ref. [25], which employs a Monte Carlo Wolff algorithm). We observe that the system first transitions to a mass superfluid state and then, at a lower temperature, transitions to a spin superfluid state, in agreement with Ref. [25]. The mass transition is predominantly determined by the superfluidity of the $m = 0$ spin component (with $m \in \{-1, 0, 1\}$ being the spin-1 magnetic sublevels). The spin transition is driven by the binding and unbinding of polar-core spin vortices (PCVs), which consist of spatially confined equal and opposite circulations in the $m = \pm 1$ components. Above the spin BKT temperature, the $m = \pm 1$ component circulations spatially separate, suggesting possible deconfinement analogous to a color plasma. We identify superfluid drag between spin components, arising from spin interactions [38–40], which we calculate analytically at zero temperature. We determine the (T, q) superfluid phase diagram for $0 < q < q_0$. At $q = 0$, the fluid response exhibits a system size dependence, suggesting the absence of a BKT transition [25]. Despite this, for finite-sized systems the decay of correlations of total spin still change from exponential to algebraic as the temperature is decreased. The decay exponent is close to 1/2 at the crossover, twice that of

U(1) systems. The recent observation of thermalization of a quasi-1D easy-plane spin-1 Bose gas [41] demonstrates that our results could be observed in current experiments.

Formalism. We use a simple-growth stochastic Gross-Pitaevskii model that couples a three-component spinor field $\Psi = (\psi_1, \psi_0, \psi_{-1})^{\mathrm{T}}$ to a grand canonical reservoir at chemical potential μ and temperature T [42–46],

$$i\hbar d\Psi = (1 - i\gamma)(\mathcal{L}\{\Psi\} - \mu\Psi)dt + i\hbar dW. \qquad (1)$$

The nonlinear operator $\mathcal{L}\{\Psi\}$ reads

$$\mathcal{L}\{\Psi\} = \left[-\frac{\hbar^2\nabla^2}{2M}\mathbb{1} + qf_z^2 + g_n n\mathbb{1} + g_s\sum_\alpha F_\alpha f_\alpha\right]\Psi \qquad (2)$$

and describes time evolution arising from the kinetic energy, quadratic Zeeman shift, density-dependent interactions (coupling constant $g_n > 0$), and spin-dependent interactions (coupling constant $g_s < 0$). Here, $n = \Psi^\dagger\mathbb{1}\Psi$ and $F_\alpha = \Psi^\dagger f_\alpha\Psi$ are the density and spin density, respectively, with $\mathbb{1}$ being the identity matrix in spin space and f_α being the spin-1 matrices ($\alpha \in \{x, y, z\}$). The dimensionless rate γ determines how strongly the system couples to the reservoir, and $dW = (dw_1, dw_0, dw_{-1})$ are Gaussian distributed complex noise terms with correlations $\langle dw_m^*(\mathbf{r})dw_{m'}(\mathbf{r}')\rangle = 2\gamma k_B T\delta(\mathbf{r} - \mathbf{r}')\delta_{m,m'}dt/\hbar$. Stationary solutions to Eq. (1) sample the grand canonical ensemble and are independent of γ [43]. In a uniform system, $q_0 = 2|g_s|n \approx 2|g_s|\mu/g_n$.

We simulate a condensate with weak spin interactions $|g_s| = 0.1g_n$ on an $N \times N$ grid with periodic boundary conditions. We use a plane-wave basis cutoff at the thermal energy k_BT [47,48]. With an adjustment to account for our use of a square grid, this gives a grid spacing $\Delta x = \sqrt{2\pi\hbar^2/Mk_BT}$. We take $\mu \approx 5q_0$ as a convenient energy scale with associated length unit $x_\mu = \hbar/\sqrt{M\mu}$. We express the temperature in terms of the dimensionless quantity $\mathcal{T} = Mg_nk_BT/\hbar^2\mu$, which captures the dependence of thermodynamic properties on both temperature and chemical potential [47,48]. Equilibrium states are obtained by evolving Eq. (1) until $t \approx 10^5\hbar/\mu$. We then evolve the equilibrium state, sampling at intervals of $10\hbar/\mu$, to build up an ensemble of $\sim 10^4$ states from which thermal averages are calculated. The system size and hence thermalization time diverge as $\mathcal{T}$ decreases; therefore we restrict our analysis to $\mathcal{T} \geqslant 0.05$.

Spin and mass BKT transitions. The two continuous symmetries in the easy-plane phase give rise to two superfluid currents at low temperatures [25]. The first is a mass superfluid current arising from the global phase coherence. The second is an F_z spin superfluid current arising from coherence of the transverse spin $\mathbf{F}_\perp = (F_x, F_y)$ [49]. The mass superfluid density can be determined from the response of the system to slowly moving boundary walls, via the current-current response tensor,

$$\chi(\mathbf{k}) = \frac{M}{k_BT}\int d^2\mathbf{r}e^{-i\mathbf{k}\cdot\mathbf{r}}\langle\mathbf{J}(\mathbf{0})\mathbf{J}(\mathbf{r})\rangle. \qquad (3)$$

Here, $\mathbf{J} = (\hbar/M)\,\mathrm{Im}(\sum_m \psi_m^\dagger\nabla\psi_m)$ is the total mass current, and angle brackets denote a thermal average. In the long-wavelength limit, the longitudinal component $\chi^L(\mathbf{k})$ of the tensor $\chi(\mathbf{k})$ is affected by the total fluid response, while the transverse component $\chi^T(\mathbf{k})$ of $\chi(\mathbf{k})$ is only affected by

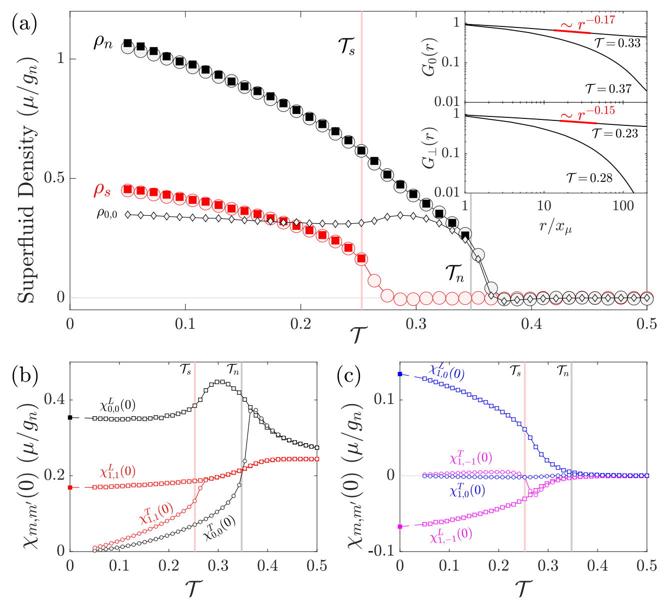

FIG. 1. (a) Mass (black circles) and F_z spin (red circles) superfluid densities, determined from Eq. (3), as a function of dimensionless temperature $\mathcal{T}$. With decreasing $\mathcal{T}$ the system first exhibits mass superfluidity and subsequently F_z spin superfluidity. The superfluid densities obtained from fitted $\eta_{n,s}$, via $\rho_{n,s} = Mk_BT/2\pi\hbar^2\eta_{n,s}$, coincide with those determined from Eq. (3) (matching black and red squares). We identify the precise BKT temperatures $\mathcal{T}_{n,s}$ to be the temperatures where $\eta_{n,s} = 1/4$. Diamonds are $\rho_{0,0}$ (see text). Inset: correlations of ψ_0 decay algebraically below the mass superfluid transition ($G_0 \sim r^{-\eta_n}$), while correlations of $\mathbf{F}_\perp$ decay algebraically below the spin superfluid transition ($G_\perp \sim r^{-\eta_s}$). Red lines are fits. (b) and (c) Transverse (circles) and longitudinal (unfilled squares) components of $\lim_{k\to 0}\chi_{m,m'}(\mathbf{k})$. Superfluid drag $\rho_{0,1}$ ($\rho_{-1,1}$) appears below $\mathcal{T}_n$ ($\mathcal{T}_s$). The analytic zero-temperature $\chi^L_{m,m'}(0)$ is indicated by filled squares. (Results are for $q = 0.03\mu \approx 0.15q_0$, $N = 256$.)

the normal fluid response [50–52]. The mass superfluid density is then $\rho_n = \lim_{k\to 0}[\chi^L(\mathbf{k}) - \chi^T(\mathbf{k})]$ (see Appendix D of Ref. [50] for details [53]). We extend this procedure to determine the F_z spin superfluid density ρ_s by considering the response to a "spin dependent" moving boundary, where the $m = \pm 1$ boundaries move in opposite directions and the $m = 0$ boundary is stationary (in experiments, this could be engineered via spin-dependent light fields [54]). We then replace $\mathbf{J}$ by $\mathbf{J}_z = (\hbar/M)\,\mathrm{Im}\,(\sum_{m,m'}\psi_m^\dagger(f_z)_{mm'}\nabla\psi_{m'})$ in Eq. (3).

In Fig. 1 we plot the mass and spin superfluid densities determined from Eq. (3). Clearly evident are the two distinct BKT temperatures $\mathcal{T}_n$ and $\mathcal{T}_s$ associated with the onset of mass and spin superfluidity, respectively. Below the mass (spin) BKT temperature, two-point correlations of ψ_0 ($\mathbf{F}_\perp$) change from decaying exponentially to decaying algebraically,

$$\begin{aligned} G_0(r) &= \frac{\langle\psi_0(\mathbf{0})^\dagger\psi_0(\mathbf{r})\rangle}{\langle\psi_0(\mathbf{0})^\dagger\psi_0(\mathbf{0})\rangle} \sim r^{-\eta_n} \quad (\mathcal{T} \leqslant \mathcal{T}_n), \\ G_\perp(r) &= \frac{\langle\mathbf{F}_\perp(\mathbf{0})\cdot\mathbf{F}_\perp(\mathbf{r})\rangle}{\langle\mathbf{F}_\perp(\mathbf{0})\cdot\mathbf{F}_\perp(\mathbf{0})\rangle} \sim r^{-\eta_s} \quad (\mathcal{T} \leqslant \mathcal{T}_s); \end{aligned} \qquad (4)$$

see inset in Fig. 1(a). The mass (spin) superfluid densities estimated from the decay exponents η_n (η_s), via $\rho_{n,s} = Mk_BT/2\pi\hbar^2\eta_{n,s}$ [30], show excellent agreement with those determined from Eq. (3); see Fig. 1. Precisely at the respective BKT temperatures the exponents take on a universal value of 1/4 [31]; hence we identify $\mathcal{T}_n$ and $\mathcal{T}_s$ in Fig. 1 as the temperatures where $\eta_{n,s} = 1/4$.

Superfluid drag. We can also examine the more general response functions

$$\chi_{m,m'}(\mathbf{k}) = \frac{M}{k_B T}\int d^2\mathbf{r}\, e^{-i\mathbf{k}\cdot\mathbf{r}}\langle \mathbf{J}_m(\mathbf{0})\mathbf{J}_{m'}(\mathbf{r})\rangle, \qquad (5)$$

with $\mathbf{J}_m = (\hbar/M)\,\mathrm{Im}(\psi_m^\dagger \nabla \psi_m)$. Note that $\chi_{m,m'} = \chi_{m',m}$ and, due to symmetry under $m = 1 \leftrightarrow m = -1$, $\chi_{m,m'} = \chi_{-m,-m'}$. Defining $\rho_{m,m'} \equiv \lim_{k\to 0}[\chi^L_{m,m'}(\mathbf{k}) - \chi^T_{m,m'}(\mathbf{k})]$, with $\chi^T_{m,m'}$ ($\chi^L_{m,m'}$) being the transverse (longitudinal) components of $\chi_{m,m'}$, the mass and spin superfluid densities can be decomposed as $\rho_n = \sum_{m,m'}\rho_{m,m'}$ and $\rho_s = \sum_{m,m'} mm'\rho_{m,m'}$. We find that mass superfluidity is primarily determined from $\rho_{0,0}$ at the mass transition; see Fig. 1(a). The transverse and longitudinal components of the four independent $\chi_{m,m'}$ are shown in Figs. 1(b) and 1(c). Off-diagonal contributions $\rho_{m,m'\neq m}$ indicate "superfluid drag" between components m and m' [55]; see Fig. 1(c). In other multicomponent systems, superfluid drag occurs via current-current coupling and is known as the Andreev-Bashkin effect [55,56], whereas in the spin-1 system it occurs due to inherent intercomponent interactions [38–40].

The zero-temperature $\chi^L_{m,m'}(0)$ can be obtained analytically as follows. Beginning with a stationary, uniform system, we impart current $(n_m\hbar k_m/M)\hat{\mathbf{x}}$ into spin component m (with $n_m = |\psi_m|^2$). Due to intercomponent interactions, this will induce currents $(n_{m'}\hbar k_{m'}/M)\hat{\mathbf{x}}$ in components $m' \neq m$. We obtain the $k_{m'\neq m}/k_m$ by minimizing the additional kinetic energy $\delta E = (\hbar^2/2M)\sum_{m'\neq m} n_{m'}k_{m'}^2$ subject to the constraint $k_1 + k_{-1} - 2k_0 = 0$ imposed by minimization of the spin-interaction energy. Defining a wave number $n_m k \equiv \sum_{m'} n_{m'}k_{m'}$ and comparing with the relation $n_m = \sum_{m'}\chi^L_{m,m'}(0)$, we surmise $\chi^L_{m,m'}(0) = n_{m'}k_{m'}/k$, where $k_{m'}/k$ has an implicit dependence on m. This is confirmed in Figs. 1(b) and 1(c).

Topological properties and confinement. In the easy-plane phase the system supports two topologically distinct vortices, associated with the U(1) and SO(2) symmetries, respectively. The destruction of mass superfluidity coincides with a proliferation of free ψ_0 vortices [see Fig. 2(a)], consistent with the finding that $\rho_n \approx \rho_{0,0}$ close to the mass BKT transition (Fig. 1). The destruction of spin superfluidity coincides with a proliferation of free $\mathbf{F}_\perp$ vortices; see Fig. 2(a). Since ψ_0 is coherent at this temperature, these circulations can be identified as PCVs, rather than Mermin-Ho vortices [57–59]. (Free vortices are identified by convolving the relevant field with a Gaussian filter before detecting divergences in the vorticity field. We choose a filter of width $5\sqrt{5}x_\mu$, which is on the order of the core size of a cold PCV [60], with $\sqrt{5}x_\mu \approx \hbar/\sqrt{2M|g_s|n}$ being the approximate spin healing length.)

A single $\mathbf{F}_\perp$ vortex consists of equal and opposite phase windings of $\psi_1\psi_0^*$ and $\psi_{-1}\psi_0^*$ bound by the spin-exchange energy $2g_s\,\mathrm{Re}\,\psi_1\psi_{-1}\psi_0^*\psi_0^*$ [57,61]. This spin-exchange energy increases linearly with separation between the $\psi_{\pm1}\psi_0^*$ vortices [62], analogous to confinement in quantum chromodynamics [63–65]. We find that the coherence between $\psi_1\psi_0^*$ and $\psi_{-1}^*\psi_0$, measured by $\langle\cos(\theta_1 + \theta_{-1} - 2\theta_0)\rangle$ (with θ_m being the phase of ψ_m), decreases with increasing temperature; see Fig. 2(a). Furthermore, there is a proliferation of free vortices in the quantity $\psi_1\psi_{-1}\psi_0^*\psi_0^*$ for $\mathcal{T} \gtrsim 0.3$ [see Figs. 2(a) and 2(b)], indicating spatial separation of $\psi_1\psi_0^*$ and $\psi_{-1}\psi_0^*$ vortices. This suggests possible PCV deconfinement, analogous to deconfinement in a color plasma. In such a plasma, this is enabled by a decrease in the strong-force coupling strength with increasing temperature [66,67]. Analogously, the spin-exchange "coupling strength" $\langle|\psi_1\psi_{-1}||\psi_0|^2\rangle$ decreases with increasing temperature; see Fig. 2(a). Ignoring fluctuations in $|\psi_0|$ and n, this coupling strength is $\propto \sqrt{n^2 - F_z^2}$ and hence diminishes with increasing fluctuations of F_z [68].

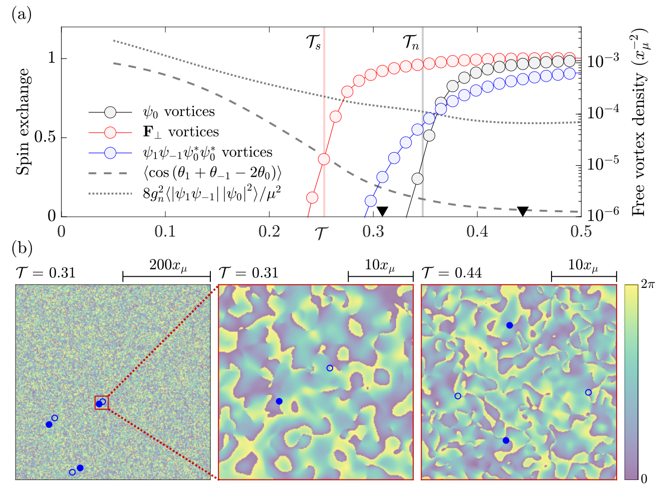

FIG. 2. (a) Right axis: Free $\mathbf{F}_\perp$ vortices proliferate for $\mathcal{T} > \mathcal{T}_s$ (red circles), which can be identified as PCVs for $\mathcal{T} < \mathcal{T}_n$. Free ψ_0 vortices proliferate for $\mathcal{T} > \mathcal{T}_n$ (black circles). Free $\psi_1\psi_{-1}\psi_0^*\psi_0^*$ vortices proliferate for $\mathcal{T} \gtrsim 0.3$ (blue circles), suggesting deconfinement of PCVs, analogous to a color plasma. Left axis: Coherence between $\psi_1\psi_0^*$ and $\psi_{-1}^*\psi_0$, measured by $\langle\cos(\theta_1 + \theta_{-1} - 2\theta_0)\rangle$ (gray dashed line), decreases with increasing temperature, along with a decrease in the "coupling strength" $\langle|\psi_1\psi_{-1}||\psi_0|^2\rangle$ (gray dotted line). (b) Profiles of $\theta_1 + \theta_{-1} - 2\theta_0$ at two temperatures [inverted triangles in (a)]. Unfilled (filled) circles denote positive (negative) free $\psi_1\psi_{-1}\psi_0^*\psi_0^*$ circulations. (Results are for $q = 0.03\mu$, $N = 256$.)

Spin and mass superfluid phase diagram. The dependence of $\mathcal{T}_n$ and $\mathcal{T}_s$ on q/μ is shown in Fig. 3(a). The linear dependence of $\mathcal{T}_s$ on q follows from evaluating the zero point of the free energy $F = E - TS$ of a single PCV, which gives $\mathcal{T}_s \propto 1 - q/q_0$ [16,69]. Here, $S = 2k_B \ln L$ and $E = \frac{K}{2}\int_{\xi_s}^{L} r^{-2}\, d^2\mathbf{r} = \pi K \ln(L/\xi_s)$ are the entropy and energy, respectively, of a single free (but confined) PCV, with L being the system size and $K \approx \hbar^2(1 - q/q_0)\mu/2g_n M$ being the spin-wave stiffness. Applying the same free-energy argument to vortices in the $m = 0$ component would give $\mathcal{T}_n \propto 1 + q/q_0$. While this qualitatively captures the increase in $\mathcal{T}_n$ with q/q_0, the linear behavior holds only for large q/q_0. The spin superfluid transition extrapolates to zero at $q = q_0$. At these low temperatures we expect ordering behavior to be affected by both quantum and thermal fluctuations [70–72].

At $q = 0$ the order parameter manifold is SO(3) [2,32], combining the symmetry of the full spin vector $\mathbf{F} = (F_x, F_y, F_z)$ and gauge symmetry into a single manifold, with

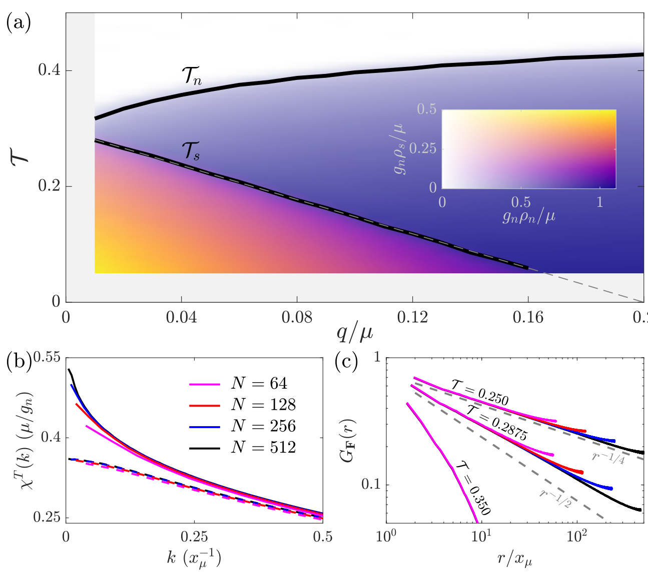

FIG. 3. (a) $(\mathcal{T}, q)$ phase diagram showing mass and spin superfluid transitions (solid black lines). The color map gives the mass and spin superfluid densities. The spin BKT temperature decreases linearly with increasing q, approaching zero as $q \to q_0$ (gray dashed line is $\propto 1 - q/q_0$ with $q_0 = 2|g_s|\mu/g_n = 0.2\mu$). Results are for $N = 256$. (b) At $q = 0$, the mass fluid response $\chi^T(k)$ (solid lines) exhibits a system size dependence. For comparison, $\chi^T(k)$ at $q = 0.01\mu$ (dashed lines) converge for increasing N. (c) Correlations of total spin, showing a crossover from exponential to algebraic decay at $\mathcal{T} \approx 0.3$ [system sizes as in (b)]. Correlations decay close to $r^{-1/2}$ at the crossover temperature. A sampling time of $2.5 \times 10^6\hbar/\mu$ is used for the $N = 512$ results in (b) and (c) to avoid autocorrelation.

vortices fundamentally distinct from U(1) systems [32]. The nature of superfluidity and the potential for BKT transitions in SO(3) systems is not well understood [25,33–37]. We find that the mass fluid response $\chi^T(k)$ exhibits a system size dependence for long wavelengths; see Fig. 3(b). This suggests the absence of a $q = 0$ mass BKT transition in the thermodynamic limit, consistent with the conclusion of Ref. [25]. Despite this, we still see a crossover from exponential to algebraic decay in correlations of total spin,

$$G_{\mathbf{F}}(r) = \frac{\langle \mathbf{F}(\mathbf{0}) \cdot \mathbf{F}(\mathbf{r})\rangle}{\langle \mathbf{F}(\mathbf{0}) \cdot \mathbf{F}(\mathbf{0})\rangle}; \quad (6)$$

see Fig. 3(c). The crossover temperature $\mathcal{T} \approx 0.3$ slowly decreases with increasing system size and hence may go to zero in the thermodynamic limit. In the finite-sized systems explored here, $G_{\mathbf{F}}(r)$ decays close to $r^{-1/2}$ at the crossover temperature, rather than as $r^{-1/4}$ typical for U(1) systems. This is similar to the scaling of low-temperature correlations in a finite-sized ferromagnetic Heisenberg model in 2D [73]. Importantly, though, the order parameter manifold of the Heisenberg model is S^2, not SO(3), and hence does not support vortices [74]. A crossover in the behavior of correlations around a well-defined temperature has been identified in a Heisenberg antiferromagnet on a triangular lattice, which also has an SO(3) order parameter manifold [36,37,75].

Discussion. In this Research Letter we identified two BKT transitions in the easy-plane phase of a ferromagnetic spin-1 Bose gas. We characterized the transitions in terms of relevant vortices and inter- and intracomponent fluid responses, and identified possible deconfinement of PCVs above the spin superfluid transition. At $q = 0$ the fluid response exhibits a system size dependence; however, correlations of total spin still exhibit a crossover from exponential to algebraic decay. It would be interesting to analyze this behavior for vanishingly small q and how this depends on system size. Extending our work, one could explore the role of nonzero axial magnetization, which adjusts the relative density of the $m = \pm 1$ spin components and modifies the nature of the PCVs [60]. One could also explore the role of transverse trapping [76], which may affect the mass and spin superfluidities differently.

Our work opens up the possibility of exploring temperature quenches across the spin BKT transition and studying nonequilibrium processes such as Kibble-Zurek scaling and coarsening dynamics. Comparisons with the extensive work on zero-temperature quenches to the easy-plane phase [6–17], particularly close to q_0, could illuminate the role of quantum versus thermal fluctuations in the symmetry breaking and nonequilibrium dynamics [70–72]. We have shown that the $m = \pm 1$ spin components decohere for increasing temperature, indicating states beyond the low-temperature U(1) × SO(2) manifold. For very high temperatures we expect restoration to the full SU(3) manifold; our work paves the way to explore how such a phase emerges.

Acknowledgments. A.J.G. acknowledges Tom Billam for useful discussions. This research was supported by the Australian Research Council Centre of Excellence for Engineered Quantum Systems (EQUS, CE170100009). This research was partially supported by the Australian Research Council Centre of Excellence in Future Low-Energy Electronics Technologies (project number CE170100039) and funded by the Australian Government. P.B.B. acknowledges support from the Marsden Fund of the Royal Society of New Zealand. X.Y. acknowledges support from the National Natural Science Foundation of China (Grant No. 12175215), the National Key Research and Development Program of China (Grant No. 2022YFA 1405300), and NSAF (Grant No. U1930403). We acknowledge the use of New Zealand eScience Infrastructure (NeSI) high-performance computing facilities.

[1] Y. Kawaguchi and M. Ueda, Spinor Bose–Einstein condensates, Phys. Rep. **520**, 253 (2012).

[2] D. M. Stamper-Kurn and M. Ueda, Spinor Bose gases: Symmetries, magnetism, and quantum dynamics, Rev. Mod. Phys. **85**, 1191 (2013).

[3] J. Stenger, S. Inouye, D. M. Stamper-Kurn, H.-J. Miesner, A. P. Chikkatur, and W. Ketterle, Spin domains in ground-state Bose-Einstein condensates, Nature (London) **396**, 345 (1998).

[4] W. Zhang, S. Yi, and L. You, Mean field ground state of a spin-1 condensate in a magnetic field, New J. Phys. **5**, 77 (2003).

[5] K. Murata, H. Saito, and M. Ueda, Broken-axisymmetry phase of a spin-1 ferromagnetic Bose-Einstein condensate, Phys. Rev. A **75**, 013607 (2007).

[6] L. E. Sadler, J. M. Higbie, S. R. Leslie, M. Vengalattore, and D. M. Stamper-Kurn, Spontaneous symmetry breaking in a quenched ferromagnetic spinor Bose–Einstein condensate, Nature (London) **443**, 312 (2006).

[7] S. R. Leslie, J. Guzman, M. Vengalattore, J. D. Sau, M. L. Cohen, and D. M. Stamper-Kurn, Amplification of fluctuations in a spinor Bose–Einstein condensate, Phys. Rev. A **79**, 043631 (2009).

[8] H. Saito and M. Ueda, Spontaneous magnetization and structure formation in a spin-1 ferromagnetic Bose–Einstein condensate, Phys. Rev. A **72**, 023610 (2005).

[9] R. Barnett, A. Polkovnikov, and M. Vengalattore, Prethermalization in quenched spinor condensates, Phys. Rev. A **84**, 023606 (2011).

[10] H. Saito, Y. Kawaguchi, and M. Ueda, Topological defect formation in a quenched ferromagnetic Bose–Einstein condensates, Phys. Rev. A **75**, 013621 (2007).

[11] A. Lamacraft, Quantum Quenches in a Spinor Condensate, Phys. Rev. Lett. **98**, 160404 (2007).

[12] B. Damski and W. H. Zurek, Dynamics of a Quantum Phase Transition in a Ferromagnetic Bose-Einstein Condensate, Phys. Rev. Lett. **99**, 130402 (2007).

[13] M. Anquez, B. A. Robbins, H. M. Bharath, M. Boguslawski, T. M. Hoang, and M. S. Chapman, Quantum Kibble-Zurek Mechanism in a Spin-1 Bose-Einstein Condensate, Phys. Rev. Lett. **116**, 155301 (2016).

[14] L. A. Williamson and P. B. Blakie, Universal Coarsening Dynamics of a Quenched Ferromagnetic Spin-1 Condensate, Phys. Rev. Lett. **116**, 025301 (2016).

[15] L. A. Williamson and P. B. Blakie, Coarsening and thermalization properties of a quenched ferromagnetic spin-1 condensate, Phys. Rev. A **94**, 023608 (2016).

[16] L. A. Williamson and P. B. Blakie, Anomalous phase ordering of a quenched ferromagnetic superfluid, SciPost Phys. **7**, 029 (2019).

[17] M. Prüfer, P. Kunkel, H. Strobel, S. Lannig, D. Linnemann, C.-M. Schmied, J. Berges, T. Gasenzer, and M. K. Oberthaler, Observation of universal dynamics in a spinor Bose gas far from equilibrium, Nature (London) **563**, 217 (2018).

[18] S. Mukerjee, C. Xu, and J. E. Moore, Topological Defects and the Superfluid Transition of the $s = 1$ Spinor Condensate in Two Dimensions, Phys. Rev. Lett. **97**, 120406 (2006).

[19] A. J. A. James and A. Lamacraft, Phase Diagram of Two-Dimensional Polar Condensates in a Magnetic Field, Phys. Rev. Lett. **106**, 140402 (2011).

[20] M. Kobayashi, M. Eto, and M. Nitta, Berezinskii-Kosterlitz-Thouless Transition of Two-Component Bose Mixtures with Intercomponent Josephson Coupling, Phys. Rev. Lett. **123**, 075303 (2019).

[21] S. S. Natu and E. J. Mueller, Pairing, ferromagnetism, and condensation of a normal spin-1 Bose gas, Phys. Rev. A **84**, 053625 (2011).

[22] Y. Kawaguchi, N. T. Phuc, and P. B. Blakie, Finite-temperature phase diagram of a spin-1 Bose gas, Phys. Rev. A **85**, 053611 (2012).

[23] K. Kis-Szabó, P. Szépfalusy, and G. Szirmai, Static properties and spin dynamics of the ferromagnetic spin-1 Bose gas in a magnetic field, Phys. Rev. A **72**, 023617 (2005).

[24] Q. Gu and R. A. Klemm, Ferromagnetic phase transition and Bose-Einstein condensation in spinor Bose gases, Phys. Rev. A **68**, 031604(R) (2003).

[25] M. Kobayashi, Berezinskii–Kosterlitz–Thouless transition of spin-1 spinor Bose gases in the presence of the quadratic Zeeman effect, J. Phys. Soc. Jpn. **88**, 094001 (2019).

[26] E. B. Sonin, Spin and mass superfluidity in a ferromagnetic spin-1 Bose-Einstein condensate, Phys. Rev. B **97**, 224517 (2018).

[27] N. D. Mermin and H. Wagner, Absence of Ferromagnetism or Antiferromagnetism in One- or Two-Dimensional Isotropic Heisenberg Models, Phys. Rev. Lett. **17**, 1133 (1966).

[28] P. C. Hohenberg, Existence of Long-Range Order in One and Two Dimensions, Phys. Rev. **158**, 383 (1967).

[29] V. L. Berezinskii, Destruction of long-range order in one-dimensional and two-dimensional systems possessing a continuous symmetry group. II. Quantum systems, J. Exp. Theor. Phys. **34**, 610 (1972).

[30] J. M. Kosterlitz and D. J. Thouless, Ordering, metastability and phase transitions in two-dimensional systems, J. Phys. C: Solid State Phys. **6**, 1181 (1973).

[31] D. R. Nelson and J. M. Kosterlitz, Universal Jump in the Superfluid Density of Two-Dimensional Superfluids, Phys. Rev. Lett. **39**, 1201 (1977).

[32] T.-L. Ho, Spinor Bose Condensates in Optical Traps, Phys. Rev. Lett. **81**, 742 (1998).

[33] H. Kawamura and S. Miyashita, Phase transition of the two-dimensional Heisenberg antiferromagnet on the triangular lattice, J. Phys. Soc. Jpn. **53**, 4138 (1984).

[34] H. Kawamura, A. Yamamoto, and T. Okubo, Z_2-Vortex ordering of the triangular-lattice Heisenberg antiferromagnet, J. Phys. Soc. Jpn. **79**, 023701 (2010).

[35] H. Kawamura and M. Kikuchi, Free-vortex formation and topological phase transitions of two-dimensional spin systems, Phys. Rev. B **47**, 1134 (1993).

[36] M. Wintel, H. U. Everts, and W. Apel, The Heisenberg antiferromagnet on a triangular lattice: topological excitations, Europhys. Lett. **25**, 711 (1994).

[37] M. Wintel, H. U. Everts, and W. Apel, Monte Carlo simulation of the Heisenberg antiferromagnet on a triangular lattice: Topological excitations, Phys. Rev. B **52**, 13480 (1995).

[38] D. V. Fil and S. I. Shevchenko, Drag of superfluid current in bilayer Bose systems, Low Temp. Phys. **30**, 770 (2004).

[39] D. V. Fil and S. I. Shevchenko, Nondissipative drag of superflow in a two-component Bose gas, Phys. Rev. A **72**, 013616 (2005).

[40] F. Carlini and S. Stringari, Spin drag and fast response in a quantum mixture of atomic gases, Phys. Rev. A **104**, 023301 (2021).

[41] M. Prüfer, D. Spitz, S. Lannig, H. Strobel, J. Berges, and M. K. Oberthaler, Condensation and thermalization of an easy-plane ferromagnet in a spinor Bose gas, Nat. Phys. **18**, 1459 (2022).

[42] C. Gardiner, J. Anglin, and T. Fudge, The stochastic Gross-Pitaevskii equation, J. Phys. B: At. Mol. Opt. Phys. **35**, 1555 (2002).

[43] C. Gardiner and M. Davis, The stochastic Gross-Pitaevskii equation: II, J. Phys. B: At. Mol. Opt. Phys. **36**, 4731 (2003).

[44] A. S. Bradley, C. W. Gardiner, and M. J. Davis, Bose-Einstein condensation from a rotating thermal cloud: Vortex

nucleation and lattice formation, Phys. Rev. A **77**, 033616 (2008).
[45] A. S. Bradley and P. B. Blakie, Stochastic projected Gross-Pitaevskii equation for spinor and multicomponent condensates, Phys. Rev. A **90**, 023631 (2014).
[46] P. B. Blakie, A. S. Bradley, M. J. Davis, R. J. Ballagh, and C. W. Gardiner, Dynamics and statistical mechanics of ultracold Bose gases using c-field techniques, Adv. Phys. **57**, 363 (2008).
[47] N. Prokof'ev, O. Ruebenacker, and B. Svistunov, Critical Point of a Weakly Interacting Two-Dimensional Bose Gas, Phys. Rev. Lett. **87**, 270402 (2001).
[48] N. Prokof'ev and B. Svistunov, Two-dimensional weakly interacting Bose gas in the fluctuation region, Phys. Rev. A **66**, 043608 (2002).
[49] The correspondence between F_z spin current and transverse spin coherence follows from noting that gradients of transverse spin angle give rise to an F_z current [77], or more formally since f_z is the generator of transverse spin rotations.
[50] C. J. Foster, P. B. Blakie, and M. J. Davis, Vortex pairing in two-dimensional Bose gases, Phys. Rev. A **81**, 023623 (2010).
[51] E. L. Pollock and D. M. Ceperley, Path-integral computation of superfluid densities, Phys. Rev. B **36**, 8343 (1987).
[52] G. Baym, The microscopic description of superfluidity, in *Mathematical Methods in Solid State and Superfluid Theory: Scottish Universities' Summer School*, edited by R. C. Clark and G. H. Derrick (Springer, Boston, 1968), pp. 121–156.
[53] We absorb a factor of k_BT into the definition of χ.
[54] F. Schmidt, D. Mayer, M. Hohmann, T. Lausch, F. Kindermann, and A. Widera, Precision measurement of the ^{87}Rb tune-out wavelength in the hyperfine ground state $f = 1$ at 790 nm, Phys. Rev. A **93**, 022507 (2016).
[55] J. Nespolo, G. E. Astrakharchik, and A. Recati, Andreev–Bashkin effect in superfluid cold gases mixtures, New J. Phys. **19**, 125005 (2017).
[56] A. F. Andreev and E. P. Bashkin, Three-velocity hydrodynamics of superfluid solutions, Sov. Phys. JETP **42**, 164 (1976).
[57] T. Isoshima, K. Machida, and T. Ohmi, Quantum vortex in a spinor Bose-Einstein condensate, J. Phys. Soc. Jpn. **70**, 1604 (2001).
[58] U. A. Khawaja and H. T. C. Stoof, Skyrmion physics in Bose-Einstein ferromagnets, Phys. Rev. A **64**, 043612 (2001).
[59] T. Mizushima, K. Machida, and T. Kita, Mermin-Ho Vortex in Ferromagnetic Spinor Bose-Einstein Condensates, Phys. Rev. Lett. **89**, 030401 (2002).
[60] L. A. Williamson and P. B. Blakie, Damped point-vortex model for polar-core spin vortices in a ferromagnetic spin-1 Bose-Einstein condensate, Phys. Rev. Res. **3**, 013154 (2021).
[61] A. M. Turner, Mass of a Spin Vortex in a Bose-Einstein Condensate, Phys. Rev. Lett. **103**, 080603 (2009).
[62] L. A. Williamson and P. B. Blakie, Dynamics of polar-core spin vortices in a ferromagnetic spin-1 Bose–Einstein condensate, Phys. Rev. A **94**, 063615 (2016).
[63] D. T. Son and M. A. Stephanov, Domain walls of relative phase in two-component Bose-Einstein condensates, Phys. Rev. A **65**, 063621 (2002).
[64] M. Tylutki, L. P. Pitaevskii, A. Recati, and S. Stringari, Confinement and precession of vortex pairs in coherently coupled Bose-Einstein condensates, Phys. Rev. A **93**, 043623 (2016).
[65] M. Eto and M. Nitta, Confinement of half-quantized vortices in coherently coupled Bose-Einstein condensates: Simulating quark confinement in a QCD-like theory, Phys. Rev. A **97**, 023613 (2018).
[66] P. Braun-Munzinger and J. Stachel, The quest for the quark–gluon plasma, Nature (London) **448**, 302 (2007).
[67] R. Pasechnik and M. Šumbera, Phenomenological review on quark-gluon plasma: Concepts vs. observations, Universe **3**, 7 (2017).
[68] Note that in the quadratic regime, fluctuations of F_z increase with increasing transverse spin disorder, since both are affected by the same Bogoliubov mode [78].
[69] J. M. Kosterlitz and D. J. Thouless, Long range order and metastability in two dimensional solids and superfluids. (Application of dislocation theory), J. Phys. C: Solid State Phys. **5**, L124 (1972).
[70] S. L. Sondhi, S. M. Girvin, J. P. Carini, and D. Shahar, Continuous quantum phase transitions, Rev. Mod. Phys. **69**, 315 (1997).
[71] M. Vojta, Quantum phase transitions, Rep. Prog. Phys. **66**, 2069 (2003).
[72] S. Sachdev, *Quantum Phase Transitions*, 2nd ed. (Cambridge University Press, Cambridge, 2011).
[73] O. Kapikranian, B. Berche, and Y. Holovatch, Quasi-long-range ordering in a finite-size 2D classical Heisenberg model, J. Phys. A: Math. Theor. **40**, 3741 (2007).
[74] H. Toda, *Composition Methods in Homotopy Groups of Spheres*, Annals of Mathematics Studies (Princeton University Press, Princeton, 1962), Vol. 49.
[75] I. S. Popov, P. V. Prudnikov, A. N. Ignatenko, and A. A. Katanin, Universal Berezinskii-Kosterlitz-Thouless dynamic scaling in the intermediate time range in frustrated Heisenberg antiferromagnets on a triangular lattice, Phys. Rev. B **95**, 134437 (2017).
[76] N. A. Keepfer, I.-K. Liu, F. Dalfovo, and N. P. Proukakis, Phase transition dimensionality crossover from two to three dimensions in a trapped ultracold atomic Bose gas, Phys. Rev. Res. **4**, 033130 (2022).
[77] E. Yukawa and M. Ueda, Hydrodynamic description of spin-1 Bose–Einstein condensates, Phys. Rev. A **86**, 063614 (2012).
[78] L. M. Symes, D. Baillie, and P. B. Blakie, Static structure factors for a spin-1 Bose–Einstein condensate, Phys. Rev. A **89**, 053628 (2014).